Parametrization of Aliphatic CH_n United Atoms of GROMOS96 Force Field

XAVIER DAURA, ALAN E. MARK, WILFRED F. VAN GUNSTEREN
Laboratorium für Physikalische Chemie, ETH Zentrum, CH-8092 Zürich, Switzerland

Received 20 July 1997; accepted 16 October 1997

ABSTRACT: The derivation of the van der Waals parameters for the aliphatic CH_n united atoms of the GROMOS96 force field is presented. The parameters have been adjusted to reproduce the experimental enthalpies of vaporization and vapor pressures or densities of a set of nine alkanes in the liquid state at 298 K (or at the boiling point in the case of methane), using a cutoff radius for the van der Waals interactions of 1.6 nm. Force fields to be used in molecular simulations are bound to the conditions chosen for their parametrization, for example, the temperature, the densities of the systems included in the calibration set, or the cutoff radius used for the nonbonded interactions. Van der Waals parameters for the CH_n united atoms of earlier GROMOS force fields were developed using a cutoff radius of 0.8 nm for the van der Waals interactions. Because the van der Waals interaction energy between aliphatic groups separated by distances between 0.8 and 1.4 nm is not negligible at liquid densities, the use of these parameters in combination with longer cutoffs leads to an overestimation of the attractive van der Waals interaction energy. The relevance of this excess attraction depends on the size of the groups that are interacting, as well as on their local densities. Free energies of hydration have been calculated for five alkanes. J Comput Chem 19: 535–547, 1998

Keywords: force field parametrization; liquid alkanes; van der Waals interactions; molecular dynamics; GROMOS96

Correspondence to: Prof. W. F. van Gunsteren; e-mail: wfvgn@igc.phys.chem.ethz.ch

Contract/grant sponsor: Swiss National Science Foundation; contract grant number 21-41875.94

CCC 0192-8651 / 98 / 050535-13

Introduction

Molecular dynamics (MD) simulations are widely used to study (bio)molecular systems at an atomic level. The quality of the information given by an MD simulation is, however, critically dependent on the way the interactions between the particles (atoms or groups of atoms) of the system are described. The size and complexity of (bio)molecular systems normally necessitate the use of empirical interaction (or potential-energy) functions to describe the interaction between the particles of the system.[1–3] The potential-energy function (or force field) is parametrized by fitting to a set of selected properties based on experimental (or *ab initio* quantum-mechanical) data for a group of model molecular systems.[3–5]

Many of the empirical force fields in general use today were initially developed by fitting parameters to experimental data such as crystal intermolecular packing, sublimation energies and dipole moments of small molecules, or to the results of molecular-orbital calculations on single molecules in the gas phase.[6–17] However, most (bio)chemical applications concern condensed-phase systems, pure liquids, solutions of organic compounds or macromolecules, and crystals. For this reason, there is an increasing trend toward the development of condensed-phase force fields that are directly parametrized to reproduce the properties of (organic) liquids, solutions, and crystals.[18–21] Although this is possibly the most direct way to achieve a self-consistent model for a given molecule, there is no guarantee that the parameters derived for pure liquids can be transferred to complex (bio)molecular systems or even transferred to the same pure liquid at a different temperature or density. Therefore, special care is needed in the choice of the molecular systems and conditions used in the parametrization procedure, and the parameters must be tested for the types of molecular systems for which the force field is intended.

The GROMOS force fields[22,23] were developed primarily for the study of biomolecules in solution (i.e., peptides and proteins, and polynucleotides). In the GROMOS87 force field[22] the CH, CH_2, and CH_3 groups were modeled as united atoms: the aliphatic and aromatic hydrogen atoms were not treated explicitly but were rather included implicitly by representing the carbon atoms and their attached hydrogen atoms as a single group centered at the carbon atom. The van der Waals parameters for these atoms were taken from the work of Dunfield et al.[24] They were derived from the calculation of crystal structures of hydrocarbons and were partially tested in similar calculations on amino acids using short (0.8-nm) nonbonded cutoff radii. In the GROMOS96 force field[23] the aliphatic CH_n groups were also represented as united atoms, but their van der Waals interactions were reparametrized on the basis of a series of MD simulations of model liquid alkanes using long (1.6-nm) nonbonded cutoff radii.

In this article we present the derivation of the van der Waals parameters for the aliphatic CH_n united atoms of the GROMOS96 force field. These parameters were adjusted to reproduce the enthalpy of vaporization and the vapor pressure (NVT) or density (NPT) of eight liquid alkanes at room temperature and methane at its boiling point. The $C12_{ii}^{1/2}$ van der Waals parameter of the water oxygen for interactions with nonpolar atoms was then adjusted to fit the experimental free energies of hydration of five of these alkanes.

Computational Methods

POTENTIAL-ENERGY FUNCTION

The standard GROMOS96 interaction function was used.[23] The terms representing the interactions between covalently connected atoms [i.e., bond stretching, bond-angle bending, harmonic (improper) dihedral-angle bending, and trigonometric dihedral-angle torsion interactions] have the form

$$\begin{aligned} V^{\mathrm{bon}}(\mathbf{r}) = & \sum_{n=1}^{N_b} \tfrac{1}{4} K_{b_n} \left[b_n^2 - b_{0_n}^2 \right]^2 \\ & + \sum_{n=1}^{N_\theta} \tfrac{1}{2} K_{\theta_n} [\cos\theta_n - \cos\theta_{0_n}]^2 \\ & + \sum_{n=1}^{N_\xi} \tfrac{1}{2} K_{\xi_n} [\xi_n - \xi_{0_n}]^2 \\ & + \sum_{n=1}^{N_\varphi} K_{\varphi_n} [1 + \cos(\delta_n)\cos(m_n \varphi_n)], \quad (1) \end{aligned}$$

where $\mathbf{r}$ is the ($3N$-dimensional) position vector of the N atoms of the system. The first summation runs over all (N_b) covalent bonds in the molecular system not treated as constraints. K_{b_n} is the force

constant, and b_n and b_{0_n} are the instantaneous and ideal lengths of bond n, respectively. The second summation runs over all (N_θ) bond angles in the molecular system. K_{θ_n} is the force constant, and θ_n and θ_{0_n} are the instantaneous and ideal values of the bond angle n, respectively. The third summation runs over a set (N_ξ) of improper dihedral angles, which are selected to keep groups of atoms near a specified spatial configuration (i.e., planar or tetrahedral). K_{ξ_n} is the force constant, and ξ_n and ξ_{0_n} are the instantaneous and ideal values of the improper dihedral angle n, respectively. The fourth summation runs over a set (N_φ) (for alkanes all) of torsional dihedral angles in the molecular system. K_{φ_n} is the force constant, δ_n is the phase shift, and m_n is the multiplicity. Table I shows the parameters used.

The terms representing the nonbonded (van der Waals and electrostatic) interactions have the form

$$V^{\text{nonb}}(\mathbf{r}) = \sum_{\substack{\text{nonbonded} \\ \text{pairs } (i,j)}} \left\{ \left[\frac{C12_{ij}}{r_{ij}^6} - C6_{ij} \right] \frac{1}{r_{ij}^6} + \frac{q_i q_j}{4\pi\varepsilon_0\varepsilon_1} \frac{1}{r_{ij}} + V^{\text{RF}}(r_{ij}, q_i, q_j, R_{\text{RF}}, \varepsilon_1, \varepsilon_2, \kappa) \right\}. \quad (2)$$

In principle, the summation runs over all atom pairs, excluding atom pairs separated by one or two covalent bonds and atom pairs separated by a distance beyond a given cutoff. The parameters $C12_{ij}$ and $C6_{ij}$ determine the van der Waals interaction between atoms i and j. In the GROMOS force field the $C12_{ij}$ and $C6_{ij}$ van der Waals parameters are defined separately for each pair of atom types. It is possible within the GROMOS force field to parametrize self-interactions (between pairs of identical atoms) separately from crossed interactions (between different atom types). The force field does not depend on a given set of combination rules, which adds considerable flexibility to the parametrization. By default, however, the parameters for crossed interactions are generated by taking the geometric mean of the self-interaction values; that is, $C12_{ij} = (C12_{ii}C12_{jj})^{1/2}$ and $C6_{ij} = (C6_{ii}C6_{jj})^{1/2}$. The $C12_{ij}$ and $C6_{ij}$ parameters can also be expressed in terms of the Lennard-Jones σ_{ij} and ε_{ij} as $C12_{ij} = 4\varepsilon_{ij}\sigma_{ij}^{12}$ and $C6_{ij} = 4\varepsilon_{ij}\sigma_{ij}^6$. q_i and q_j are the (partial) charges of atoms i and j, ε_0 is the dielectric permittivity of the vacuum, ε_1 is the relative dielectric permittivity within the sphere of radius R_c (cutoff radius) centered in atom i ($\varepsilon_1 = 1$ in the GROMOS force field), and r_{ij} is the distance between atoms i and j. The electrostatic interactions beyond the cutoff are approximated by a Poisson–Boltzmann generalized reaction field term V^{RF}.[23] This term represents the force on atom i due to the reaction field induced by atom j when assuming an electrostatic continuum characterized by a relative dielectric permittivity ε_2 (reaction field permittivity) and an inverse Debye screening length κ outside the reaction field cutoff radius R_{RF}.

PARAMETRIZATION PROCEDURE

The partial charges on the united CH_n atoms of the alkanes were set to zero. To derive the $C12_{ii}^{1/2}$ and $C6_{ii}^{1/2}$ van der Waals parameters for CH, CH_2, CH_3, and CH_4, a series of NVT MD simulations were performed on nine model alkanes in the liquid state: methane, ethane, propane, butane, isobutane, pentane, isopentane, cyclopentane, and

TABLE I.
Parameters Used for Calculation of Interactions Between Covalently Connected Atoms.

Interaction	Force Constant	Ideal Value
CH_n–CH_n (bonds)	$K_{b_n} = 7.15 \times 10^6$ kJ mol^{-1} nm^{-4}	$b_{0_n} = 0.153$ nm
CH_n–CH_n–CH_n (bond angles)	$K_{\theta_n} = 530$ kJ mol^{-1}	$\theta_{0_n} = 111°$
Tetrahedral centers (improper dihedral angles)	$K_{\xi_n} = 0.102$ kJ mol^{-1} degree^{-2}	$\xi_{0_n} = 35.264°$
CH_n–CH_n–CH_n–CH_n (torsional dihedral angles)	$K_{\varphi_n} = 5.86$ kJ mol^{-1}	—[a]

Parameters taken from the GROMOS96 force field.[23]
[a] The phase shift δ_n is 0, and the multiplicity is 3.

cyclohexane. The experimental observables used to parametrize the model systems were the enthalpy of vaporization (ΔH_{vap}) and the vapor pressure (vap P) of the liquids at 298 K (or at the boiling point in the case of methane). The enthalpy of vaporization was calculated using the relation

$$\Delta H_{vap} = E_{intra}(g) - [E_{inter}(l) + E_{intra}(l)] + RT, \quad (3)$$

where E_{intra} is the intramolecular energy per molecule [calculated for both the gas (g) and the liquid (l) states] and E_{inter} is the intermolecular energy per molecule. RT is equal to the pressure–volume term in $H = E + PV$, assuming an ideal gas. Assuming that the sum of (quantum) kinetic and vibrational energies is equal for the gas and liquid states,[25] the following expression for ΔH_{vap} in terms of the potential energy is obtained:

$$\Delta H_{vap} = V_{intra}(g) - [V_{inter}(l) + V_{intra}(l)] + RT. \quad (4)$$

To parametrize the models, an extensive search of σ_{ii} and ε_{ii} values for each of the four united atoms was performed with the aim to fit the enthalpy of vaporization and the pressure of the model systems to the experimental values. For the united atom models under study, the enthalpy of vaporization and the pressure approximately follow isoenergies and isobars in the plane defined by σ and ε. The parametrization was performed in two stages. An initial set of $C12_{ii}^{1/2}$ and $C6_{ii}^{1/2}$ parameters were obtained treating each of the united atoms independently. The CH_4 was parametrized on methane. The CH_2 was parametrized on cyclopentane and cyclohexane. The CH_3 was parametrized on butane and isobutane, using fixed parameters for the CH_2 (from cyclopentane and cyclohexane) and the CH (from the OPLS force field[19]). A 200-ps simulation was performed for each σ_{ii} ε_{ii} pair tested, and the enthalpy of vaporization and pressure were evaluated from the last 150 ps of the trajectory. This procedure was iterated until the σ_{ij} and ε_{ii} parameters converged. After this initial parametrization cycle, the $C12_{ii}$ and $C6_{ii}$ parameters for CH, CH_2, and CH_3 were further tuned using all the alkanes in the calibration set, with the exception of methane. For each new set of σ_{ii} and ε_{ii} parameters tested, the alkane systems affected were simulated for 200 ps, and the new parameters accepted when the sum of the differences between the enthalpies of vaporization and between the vapor pressures from the model and experiment for all compounds reached a minimum. The aim was to achieve a compromise between the properties of each of the nine model alkane systems. The parametrization of van der Waals interactions is, however, highly dependent on the density of the system under study. Thus, for parametrization purposes one should choose, as far as possible, systems with densities in a range similar (at the same temperature) to that of the systems for which the force field is developed (i.e., biomolecules). For this reason, the liquids with higher densities at 298 K (butane, isobutane, pentane, isopentane, cyclopentane, and cyclohexane) were given more weight in the parametrization procedure.

As stated earlier, in the GROMOS force field the van der Waals interaction parameters are defined separately for each pair of atom types. To avoid individually parametrizing all cross terms, different $C12_{ii}^{1/2}$ parameters are used in conjunction with the default (geometric) combination rules, depending on the nature of the interaction. For example, the $C12_{ii}^{1/2}$ parameter of the water oxygen for its interactions with nonpolar atoms is to be parametrized against the most representative nonpolar atoms of the force field, that is, the united CH_n atoms. We extrapolated the parameter $C12_{OwOw}^{1/2}$ for interactions with nonpolar atoms from the calculation of the free energy of hydration of methane, ethane, propane, butane, and isobutane at two different $C12_{OwOw}^{1/2}$ values, assuming that for these solutes $\Delta G_{hyd}(C12_{OwOw}^{1/2})$ is approximately a linear function.

MD SIMULATIONS OF MODEL LIQUID ALKANES

Molecular Models

All internal interactions (except bond stretching) were considered explicitly. Improper dihedral angles were used in isobutane and isopentane to keep the respective CH centers in a tetrahedral configuration. Intramolecular 1–2 and 1–3 van der Waals interactions, between atoms connected through one and two bonds, respectively, were excluded. Special (lower) $C12_{ii}^{1/2}$ and $C6_{ii}^{1/2}$ parameters (common for the GROMOS87 and GROMOS96 force fields) were used for the 1–4 van der Waals interactions in butane, pentane, isopentane, and cyclohexane. The 1–4 $C12_{ii}^{1/2}$ was 1304.0 and 1698.0 (kcal mol^{-1} Å^{12})$^{1/2}$ for CH_2 and CH_3, respectively, and the 1–4 $C6_{ii}^{1/2}$ was 33.60 and 40.47 (kcal mol^{-1} Å^{6})$^{1/2}$ for CH_2 and CH_3, respectively.

The 1–5 van der Waals interactions in pentane were treated as normal interactions. In all cases except pentane a single charge group was defined per molecule and used for the generation of a charge-group based pair list. For pentane, three charge groups were defined (2-1-2).

Each system consisted of a cubic box containing 512 molecules at the experimental density of the liquid at 298 K (or at the boiling point in the case of methane and in one of the simulations of ethane).

NVT and NPT Simulations

Initial velocities were taken from a Maxwellian distribution at 298 K. Rectangular periodic boundary conditions were applied. The system was weakly coupled to a temperature of 298 K with a relaxation time of 0.1 ps.[26] In the NPT simulations the system was, in addition, weakly and anisotropically coupled to the experimental pressure with a relaxation time of 0.5 ps.[26] Bond lengths were constrained to equilibrium values using the SHAKE algorithm,[27] with a geometric tolerance of 10^{-4}. The time step for the leapfrog integration scheme was set to 0.002 ps. The van der Waals interactions were evaluated at every time step using a charge-group pair list that was updated every 10 time steps with a cutoff radius of 1.6 nm (1.4 nm in the simulations of liquid methane). The cutoff radius was applied to the centers of geometry of the charge groups. The NVT simulations consisted of 50-ps equilibration and 150-ps data collection. The NPT simulations were started from the end configurations and velocities of the corresponding NVT simulations and were run for 300 ps (100 ps for equilibration and 200 ps for data collection). Variations to these settings are discussed where appropriate in the text.

Vacuum Simulations

Simulations in the gas state were performed to compute the internal potential energy, the $V_{\text{intra}}(g)$ term in eq. (4). There is no vacuum correction for either methane or ethane, because these systems lack intramolecular interactions. The vacuum simulations were started from the end configurations and velocities of the corresponding NVT simulations. All intermolecular interactions were disabled, the geometric tolerance for SHAKE was reduced to 10^{-8} to strictly ensure energy conservation, and the systems were then simulated for 100 ps without temperature coupling. The average temperature remained around 298 K.

CALCULATION OF FREE ENERGIES OF HYDRATION

Free-Energy Differences by Thermodynamic Integration

The difference in free energy between two states A and B of a molecular system, with interaction functions denoted by $V_A(\mathbf{r})$ and $V_B(\mathbf{r})$, may be expressed as[28]

$$\Delta G_{BA} = G_B - G_A = \int_{\lambda_A}^{\lambda_B} \left\langle \frac{\partial V(\mathbf{r}; \lambda)}{\partial \lambda} \right\rangle_{\lambda'} d\lambda', \quad (5)$$

where $\mathbf{r}$ is the ($3N$-dimensional) position vector of the N atoms of the system, and $V(\mathbf{r}; \lambda)$ is a potential energy function parametrized by the coupling variable λ, continuous in λ, and satisfying

$$V(\mathbf{r}; \lambda_A) = V_A(\mathbf{r}) \quad \text{and} \quad V(\mathbf{r}; \lambda_B) = V_B(\mathbf{r}). \quad (6)$$

The angle brackets in (5), $\langle \cdots \rangle_{\lambda'}$, denote averaging over an equilibrium ensemble generated with the potential energy function $V(\mathbf{r}; \lambda')$. If MD simulations are used to generate the ensembles of molecular configurations, the integral in (5) can be evaluated in different ways. In the slow-growth method the coupling parameter λ is made a function of time and slowly changed from λ_A to λ_B during the course of a simulation. In the multiconfiguration thermodynamic-integration method the ensemble average in (5) is evaluated at a number of discrete λ' points by performing a separate simulation at each chosen λ' point. The integral is then determined numerically.

Thermodynamic Cycle

The thermodynamic cycle used to calculate the free energies of hydration is represented in Figure 1. The free energy of hydration is the work required to transfer a molecule from the gas state to water, which is ΔG_1 in Figure 1. ΔG_1 was not determined directly but estimated from $\Delta G_1 = \Delta G_2 + \Delta G_3 - \Delta G_4$. ΔG_4 is the work required to remove all interactions between the solute and the solvent. In the cases under study it is sufficient to remove the van der Waals interactions between the alkane and the water molecules. ΔG_3 is the work required to transform the alkane into a dummy alkane in a vacuum. Because all intramolecular interactions were unchanged, $\Delta G_3 = 0$. ΔG_2 is the work required to transfer the dummy

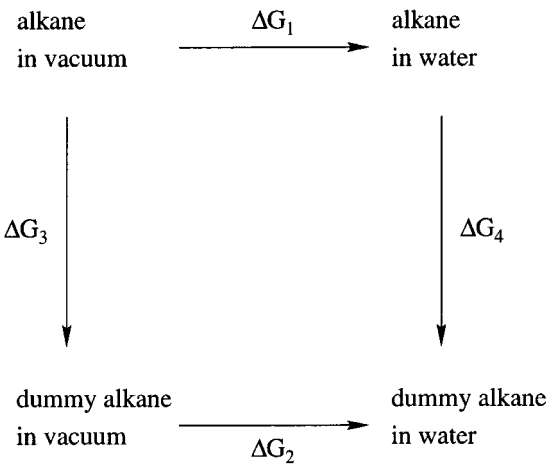

FIGURE 1. Thermodynamic cycle used for the calculation of the free energies of hydration of methane, ethane, propane, butane, and isobutane. A dummy alkane is here defined as not having intermolecular interactions. The free energy of hydration (ΔG_1) is calculated as $\Delta G_1 = \Delta G_2 + \Delta G_3 - \Delta G_4$.

alkane from the vacuum to water (again zero). As ΔG_2 and ΔG_3 are zero, ΔG_1 is equal to $-\Delta G_4$. Note that only intermolecular interactions are changed. If any of the intramolecular interactions of the alkane, including the 1–4 van der Waals interaction in the case of butane, were perturbed in the course of the mutation to determine ΔG_4 and ΔG_3, ΔG_3 would not be zero and would have to be calculated.

λ Dependence of Potential-Energy Function

The van der Waals term of the λ-dependent version of the interaction function of GROMOS96[23] was used. This so-called soft-core interaction function does not diverge at small interparticle distances (no singularity at $r_{ij} = 0$) and allows for a smooth mutation of real atoms to dummy atoms and *vice versa*. This van der Waals λ-dependent interaction function reads

$$V^{\mathrm{LJ}}(\mathbf{r};\lambda) = \sum_{\substack{\text{nonbonded}\\ \text{perturbed pairs}(i,j)}} \left\{ (1-\lambda)^n \left[\frac{C12_{ij}^A}{\alpha_{ij}^{\mathrm{LJ}}\lambda^2\left(\sigma_{ij}^A\right)^6 + r_{ij}^6} - C6_{ij}^A \right] \frac{1}{\alpha_{ij}^{\mathrm{LJ}}\lambda^2\left(\sigma_{ij}^A\right)^6 + r_{ij}^6} + \lambda^n \left[\frac{C12_{ij}^B}{\alpha_{ij}^{\mathrm{LJ}}(1-\lambda)^2\left(\sigma_{ij}^B\right)^6 + r_{ij}^6} - C6_{ij}^B \right] \frac{1}{\alpha_{ij}^{\mathrm{LJ}}(1-\lambda)^2\left(\sigma_{ij}^B\right)^6 + r_{ij}^6} \right\}, \tag{7}$$

where

$$n = 1, \quad \alpha_{ij}^{\mathrm{LJ}} = 0.5,$$

$$\left(\sigma_{ij}^X\right)^6 = \begin{cases} \dfrac{C12_{ij}^X}{C6_{ij}^X} & \text{if } C6_{ij}^X \neq 0 \\ 0 & \text{if } C6_{ij}^X = 0 \end{cases}. \tag{8}$$

The summation in (7) runs over all atom pairs that involve at least one perturbed atom and for which the interaction is calculated. The van der Waals interaction between nonperturbed atoms is evaluated using (2).

Simulation Setup

The alkane was placed in the center of a periodic rectangular box, chosen such that the minimum distance from any solute atom to the wall was 1.5 nm. The box was then filled with an equilibrated configuration of SPC[18] water molecules, and all water molecules with the oxygen atom lying within 0.23 nm of a solute atom were removed. Slow-growth simulations were used to generate the initial configurations for the simulations at different λ' values. The solute and the solvent were independently, weakly coupled to a temperature of 298 K with a relaxation time of 0.1 ps. The entire system was weakly, anisotropically coupled to a pressure of 1 atm with a relaxation time of 0.5 ps. The nonbonded interactions were evaluated using a twin-range cutoff (0.8/1.4 nm). All other parameters were as described previously. The coupling parameter λ was changed from $\lambda_A = 0$ to $\lambda_B = 1$ in 200 ps. Eighteen λ' points were chosen at which ensemble averages for thermodynamic integration were calculated. The same parameter settings described before for the slow-growth simulations were used in the (NPT) simu-

lations at discrete λ' points. At each λ' point the system was equilibrated for a minimum of 20 ps. Simulations of 50–350 ps were used to calculate the ensemble averages $\langle \partial V/\partial\lambda \rangle_{\lambda'}$. The sampling time at each λ' point depended on the convergence properties of $\langle \partial V/\partial\lambda \rangle_{\lambda'}$.

Integration and Calculation of Errors

The error in $\langle \partial V/\partial\lambda \rangle_{\lambda'}$ was estimated from its standard deviation $\sigma(\langle \partial V/\partial\lambda \rangle_{\lambda'})$ as described by Fincham et al.[29] and Allen and Tildesley.[30] The trapezoid method was used to integrate $\langle \partial V/\partial\lambda \rangle_{\lambda'}$ numerically between 0 and 1. To estimate the error in ΔG due to the trapezoidal integration, $\langle \partial V/\partial\lambda \rangle_{\lambda'}$ was assumed to be Gaussian distributed with a maximum probability equal to $\langle \partial V/\partial\lambda \rangle_{\lambda'}$ and a width of $\sigma(\langle \partial V/\partial\lambda \rangle_{\lambda'})$. The distributions were assumed to be uncorrelated among different λ' points. The standard deviation on ΔG was then calculated as[31]

$$\sigma(\Delta G) = \left[\sum_{n=1}^{N_\lambda} w(\lambda_n) \sigma^2(\langle \partial V/\partial\lambda \rangle_{\lambda_n}) \right]^{1/2}, \quad (9)$$

where N_λ is the number of λ' points at which the ensemble average has been calculated, $w(\lambda_n)$ is the weight factor from the trapezoidal integration, and $\sigma(\langle \partial V/\partial\lambda \rangle_{\lambda_n})$ is the error in the ensemble average.

Results and Discussion

OPTIMIZED PARAMETERS

The σ_{ii} and ε_{ii} van der Waals parameters, as well as the corresponding $C6_{ii}^{1/2}$ and $C12_{ii}^{1/2}$, obtained in this work for the united atoms CH, CH_2, CH_3, and CH_4 of the GROMOS96 force field are shown in Table II. The GROMOS87 and OPLS parameters are also shown for comparison. The van der Waals parameters for the united CH_n atoms of GROMOS96 are in general much closer to the OPLS values than the corresponding GROMOS87 parameters. This is primarily a reflection of the cutoff radius used for the parametrization. The GROMOS87 parameters perform better using a 0.8-nm van der Waals cutoff. The OPLS parameters were also obtained with a short cutoff,[19] but they incorporated a tail correction. Such a tail correction cannot be easily transferred to mixed systems. Contrary to the OPLS force field, in the GROMOS96 force field a single type of CH_3 united atom is used.

Table III shows the computed values for the density, enthalpy of vaporization, and vapor pressure of the model liquid alkanes when using the GROMOS87 (NVT simulations), OPLS (NVT simulations), and GROMOS96 (NVT and NPT simulations) van der Waals parameters, as well as the

TABLE II.
van der Waals Parameters for the CH_n United Groups in GROMOS87,[22] OPLS,[19] and GROMOS96[23] Force Fields.

Group	Force Field	σ (Å)	ε (kcal mol^{-1})	$C6_{ii}^{1/2}$ (kcal mol^{-1} Å^6)$^{1/2}$	$C12_{ii}^{1/2}$ (kcal mol^{-1} Å^{12})$^{1/2}$
CH	GROMOS87	4.232	0.130	54.65	4141.0
	OPLS	3.850	0.080	32.28	1842.2
	GROMOS96	3.800	0.075	30.05	1649.2
CH_2	GROMOS87	3.965	0.140	46.63	2906.0
	OPLS	3.905	0.118	40.91	2436.1
	GROMOS96	3.920	0.117	41.21	2482.2
CH_3	GROMOS87	3.786	0.180	46.06	2500.0
	OPLS (—CH_3)[a]	3.775	0.207	48.95	2633.4
	OPLS (—CH_2)[b]	3.905	0.175	49.82	2966.7
	OPLS (—CH)[c]	3.910	0.160	47.82	2858.6
	GROMOS96	3.875	0.175	48.68	2832.6
CH_4	GROMOS87	—	—	—	—
	OPLS	3.730	0.294	56.28	2920.5
	GROMOS96	3.710	0.302	56.12	2866.0

[a] CH_3 bound to a CH_3.
[b] CH_3 bound to a CH_2.
[c] CH_3 bound to a CH.

TABLE III.
Density (ρ, kg m^{-3}), Vapor Pressure (vap P, atm), and Heat of Vaporization (ΔH_{vap}, kJ mol^{-1}) of Model Liquid Alkanes Studied at 298 K Using GROMOS96 Force Field.

Case	ρ	vap P	ΔH_{vap}	ρ	vap P	ΔH_{vap}	ρ	vap P	ΔH_{vap}	ρ	vap P	ΔH_{vap}	ρ	vap P	ΔH_{vap}
	Methane[b]			Ethane[b]			Ethane			Propane			*n*-Butane		
Experimental[a]	424	1	8.19	546	1	14.70	315	41	5.16	493	9	14.79	573	2	21.62
GROMOS87 (NVT)					357	12.75		107	8.58		−33	16.09		−227	23.07
OPLS (NVT)		121	8.06		36	14.57		25	9.67		165	15.65		117	21.56
GROMOS96 (NVT)		2	8.18		812	13.11		134	8.83		138	15.45		77	21.31
GROMOS96 (NPT)	424	1	8.18				76	43	4.26	449	10	14.32	557	2	20.80
	Isobutane			*n*-Pentane			Isopentane			Cyclopentane			Cyclohexane		
Experimental[a]	551	3	19.23	621	0.7	26.43	614	0.9	24.85	741	0.4	28.53	774	0.1	33.04
GROMOS87 (NVT)		−376	23.66		−388	29.77		−608	30.30		−245	34.55		−510	41.69
OPLS (NVT)		108	18.85		18	26.94		25	24.81		54	27.64		−129	33.38
GROMOS96 (NVT)		5	19.54		−18	26.77		−56	25.02		117	27.74		−44	33.53
GROMOS96 (NPT)	551	3	19.54	624	1	26.92	623	1	25.37	730	1	27.34	791	1	34.07

This is a comparison with experimental data and with results obtained with the GROMOS87 and OPLS van der Waals parameters (cutoff radius 1.6 nm).
[a] Experimental data from ref. 33.
[b] At the boiling point (111.66 K for methane and 184.52 K for ethane).

corresponding experimental values. Note that all the computational results presented in this table were obtained using the GROMOS96 MD simulation programs[23] under the same conditions. The results obtained with the OPLS van der Waals parameters may not be identical to the results obtained using the BOSS program.[32] For example, the pressure is calculated using a different algorithm and no tail correction has been applied to the van der Waals interactions in GROMOS96. From Table III it is obvious that it is not possible to simultaneously fit the density, pressure, and ΔH_{vap} for all the alkanes tested using just four united atom types. However, the inclusion of additional atom types as in the OPLS force field does not significantly improve the overall fit. The pressure (NVT) or density (NPT) was most sensitive to changes in the parameters. Methane was simulated at its boiling point (111.66 K). Both the GROMOS96 and the OPLS CH_4 were parametrized at this temperature. Liquid ethane was simulated at the boiling point (184.52 K) and at 298 K. The OPLS CH_3 for ethane (see Table II) was parametrized at the boiling point and gives good agreement with the experiment at this temperature. The GROMOS96 model liquid ethane is approximately 1.5 kJ mol^{-1} too low in energy and the pressure is 812 atm. At 298 K both ethane models failed to reproduce the experimental enthalpy of vaporization. This simply illustrates the strong dependence of the parametrization on the temperature (and density) of the system. In view of these results, an extensive search of σ_{ii} and ε_{ii} parameters was performed in an attempt to obtain CH_3 parameters specific for liquid ethane at 298 K. However, no combination of σ_{ii} and ε_{ii} values that simultaneously reproduced the experimental ΔH_{vap} and vap P was found. A 6–12 Lennard–Jones interaction function, together with a united atom model, is not appropriate for liquid ethane at room temperature. The remaining model liquid alkanes were studied at 298 K. In general, the GROMOS87 parameters produced too low pressures and too high energies when a cutoff radius of 1.6 nm was used. There were no major differences between the results obtained with the OPLS and the GROMOS96 parameters, as expected from the small differences in the parameters (see Table II). There is apparently no major advantage in using multiple CH_3 united atom types as in the OPLS force field, except in the case of ethane, which is not relevant for biomolecular simulations. The enthalpies of vaporization obtained with the GROMOS96 force field differ in all cases by less than 1 kJ mol^{-1} from the experimental ones. In the NPT simulations the density was in all cases within 3% of the

experimental value, except for propane, for which the density was 9% lower than the experimental one. Due to the changes in density, the enthalpies of vaporization calculated from the NPT simulations were slightly different from the ones calculated from the NVT simulations, but they still differ from the experimental values by less than 1.2 kJ mol^{-1}. Cyclopentane and cyclohexane illustrate the intrinsic difficulty of deriving multipurpose atom types. The GROMOS96 CH_2 model gives a higher vapor pressure and a slightly lower enthalpy of vaporization than the experiment in the case of cyclopentane and the opposite in the case of cyclohexane. It is thus not possible to exactly reproduce the properties of both model liquids at the same time using a single model CH_2.

DEPENDENCE OF VAN DER WAALS INTERACTION ENERGY ON CUTOFF RADIUS

It has been commonly assumed in force fields designed for biological systems that van der Waals interactions at distances longer than 0.8 nm can be neglected without seriously affecting the properties of the system. In general, this is not true. Table IV shows the enthalpies of vaporization and vapor pressures of the model liquid alkanes studied, calculated from NVT simulations in which the GROMOS96 force field and different cutoff radii were used, as well as the corresponding experimental values. It is evident from Table IV that the parametrization will be highly dependent on the cutoff radius used for the van der Waals interactions. The effect is extremely important for cutoff radii between 0.8 and 1.4 nm, but it reaches a plateau for cutoff radii between 1.6 and 1.8 nm, depending on the case. The effect of the cutoff is greater as the density and the size of the molecule increase. The enthalpy of vaporization is a molecular quantity. For every molecule that falls within the cutoff sphere around a given central molecule, 1 interaction is gained in the case of methane, 4 interactions in the case of ethane, 9 in the case of propane, 16 in the case of isobutane, and so on. A similar dependence is observed with the pressure of the system, which is also a function of the number of intermolecular interactions. Such effects can be corrected using a tail correction, but only in the case of a homogeneous system, not, for example, in a solvated protein.

The effect of having defined a single charge group per molecule (except for pentane for which three charge groups were defined) for the search of

TABLE IV.
Dependence of Vapor Pressure (vap P, atm) and Enthalpy of Vaporization (ΔH_{vap}, kJ mol^{-1}) on Cutoff Radius Used for van der Waals Interactions.

	Methane		Ethane		Propane		*n*-Butane		Isobutane		*n*-pentane		Isopentane		Cyclopentane		Cyclohexane	
R_c	vap P	ΔH_{vap}	vap P	ΔH_{vap}	vap P	ΔH_{vap}	vap P	ΔH_{vap}	vap P	ΔH_{vap}	vap P	ΔH_{vap}	vap P	ΔH_{vap}	vap P	ΔH_{vap}	vap P	ΔH_{vap}
0.8	367	7.48	314	7.83	597	13.22	810 (615)	17.77 (18.50)	501	16.31	639	22.82	776	20.59	954	23.33	758	27.81
1.0	145	7.90	214	8.39	351	14.49	393 (323)	19.76 (20.11)	238	18.08	275	25.07	276	23.00	552	25.55	302	30.46
1.2	48	8.09	170	8.64	234	15.07	211 (191)	20.67 (20.74)	112	18.99	111	26.05	85	24.19	272	26.85	90	32.37
1.4	2	8.18	145	8.75	173	15.31	132 (121)	21.13 (21.14)	31	19.32	36	26.54	0	24.71	173	27.41	17	33.11
0.8 / 1.4[a]	−3	8.18	147	8.75	180	15.33	128	21.14	30	19.34	35	26.57	−15	24.73	192	27.42	36	33.21
1.6			134	8.83	138	15.45	77 (80)	21.31 (21.33)	5	19.54	−18	26.77	−56	25.02	117	27.74	−44	33.53
1.8			123	8.85	126	15.54	52	21.44	−30	19.64	−45	27.00	−74	25.25	74	27.88	−75	33.77
Exptl.[b]	1	8.19	41	5.16	9	14.79	2	21.62	3	19.23	0.7	26.43	0.9	24.85	0.4	28.53	0.1	33.04

These are results from a series of NVT simulations (of length 150 ps) using the GROMOS96 force field. Cutoff distance, R_c, in nanometers. Values in parentheses correspond to simulations of butane with four charge groups per molecule (one per united atom).

[a] Twin-range cutoff.

[b] Experimental data from ref. 33.

neighbors (generation of the charge-group pair list) was also studied. The molecules potentially most affected are butane and isopentane. A second set of simulations with different cutoff radii were performed for butane, with four charge groups (one per united atom) per molecule. The results are shown in parentheses in Table IV. The effect of the number of charge groups per molecule is only important when using a cutoff radius of 0.8 nm. For a cutoff of l.0 nm the effect is minor, and at 1.6 nm the effect is insignificant. Larger charge groups improve the efficiency of the pair-list generation. The parametrization of the GROMOS96 van der Waals CH_n interactions was performed using a cutoff of 1.6 nm. This avoided the need for long-range (tail) corrections, and the results using this cutoff were not significantly affected by the number of charge groups defined per molecule. The data shown in Table IV indicate that the GROMOS96 van der Waals parameters for the CH_n united atoms can be used with a cutoff of 1.4 nm or higher for the calculated ΔH_{vap} and vap P to be close to the experimental values. [Note, e.g., butane in Table III, that a difference in vapor pressure with the experiment of 75 atm in simulation GROMOS96 (NVT) corresponds to a difference in density with the experiment in simulation GROMOS96 (NPT) of only 2.8%.] Because using a single cutoff of 1.4 nm is computationally expensive, the use of a twin-range cutoff (0.8/1.4 nm) for the van der Waals interactions, in which the short-range interactions ($r \leq 0.8$ nm) are determined every step but the longer range interactions (0.8 nm $< r \leq 1.4$ nm) are only updated with the pair list, was also tested. The results are shown in Table IV. There is almost no difference from the results obtained with the single cutoff at 1.4 nm. The effect of the number of steps between updates of the charge-group pair list was also studied for butane (results not shown). In the simulations already presented, the pair list was updated every 10 time steps. Updating the charge-group pair list every time step, with a cutoff radius of 1.6 nm, gave a vap P of 95 atm when one charge group per butane molecule was defined and 72 atm when four charge groups per molecule were defined, and a ΔH_{vap} of 21.31 and 21.37 kJ mol^{-1}, respectively. Thus, there is little difference in the pressures and no difference in the enthalpies of vaporization caused by the different frequencies of the updates. The long-range van der Waals interaction is primarily a function of the local density. Because the local density changes slowly on the MD time scale, updating the long-range van der Waals interactions only every 10 steps results in no significant effect.

To give an idea of the range of variation of the density with the cutoff radius, a series of NPT simulations of isobutane with different cutoff radii were performed. The results are shown in Table V. As in the NVT simulations, the effect of the cutoff is very important for cutoff radii between 0.8 and 1.4 nm. With a cutoff radius of 0.8 nm the system continuously expanded (evaporated) due to a critical loss of interaction energy.

FREE ENERGIES OF HYDRATION

The $C12^{1/2}_{OwOw}$ parameter of the GROMOS96 force field for interactions of water with nonpolar atoms was extracted from the calculation of the free energy of hydration of methane, ethane, propane, butane, and isobutane by interpolating between two of different $C12^{1/2}_{OwOw}$ values of 421 and 793 (kcal mol^{-1} Å^{12})$^{1/2}$, assuming that for these solutes $\Delta G_{hyd}(C12^{1/2}_{OwOw})$ is linear. The value obtained was 755 (kcal mol^{-1} Å^{12})$^{1/2}$. The free energies of hydration of the five model alkanes were then computed again using this new parameter value. The results are shown in Table VI. Free energies of hydration reported by Kaminski et al.[20] (all except for isobutane) using the OPLS force field and the TIP4P water model[34] are also shown for comparison. Note that Kaminski et al.[20] calculated the free energies of hydration by summing the perturbations in water of butane to propane, propane to ethane, ethane to methane, and the final annihilation of methane. Table VII shows the details of our simulations. The results obtained are in good quantitative agreement with the experimental free energies of hydration. With the excep-

TABLE V.
Example of Dependence of Density (ρ, kg m^{-3}) on Cutoff Radius (R_c, nm) Used for van der Waals Interactions.

	Isobutane		
R_c	ρ	vap P (atm)	ΔH_{vap} (kJ mol^{-1})
0.8[a]	—	—	—
1.0	468	3	15.65
1.2	521	3	18.05
1.4	542	5	19.05
1.6	551	3	19.54

[a] Using a cutoff of 0.8 nm, we could not get a stable density (i.e., the system continuously expands).

TABLE VI.
Free Energies of Hydration of Five of Model Alkanes Studied, Calculated with GROMOS96 Force Field.

Compound	ΔG_{hyd} (kJ mol^{-1})			
	Experimental[a]	GROMOS96	OPLS[b,c]	OPLS[b,d]
Methane	8.37	8.0 ± 1.3	10.3	9.2
Ethane	7.66	9.2 ± 2.1	9.7	8.2
Propane	8.19	9.0 ± 2.2	13.8	9.1
Butane	8.70	7.7 ± 2.2	15.0	10.3
Isobutane	9.70	10.4 ± 2.2		

This is a comparison with values reported by Kaminski et al.[20] using the OPLS united atom and all atom force fields.
[a] Data from ref. 35 and 36.
[b] Data from ref. 20.
[c] United atom model.
[d] All atom model.

tion of ethane, for which no reasonable united atom model at 298 K could be obtained, the calculations agree within 1 kJ mol^{-1} with the experiment. The relative differences between the free energies of hydration of the five model alkanes are, however, not the same as found experimentally in all cases. Because the differences in free energy of hydration between the five alkanes are smaller than the estimated errors, it is not possible to say if this is due to inadequacy of the force field or the molecular model (e.g., united-atom vs. all-atom models) or simply due to insufficient sampling.

Conclusions

The derivation of the van der Waals parameters for the aliphatic CH_n united atoms of the GROMOS96 force field has been presented. The parameters have been adjusted to reproduce the experimental enthalpies of vaporization and vapor pres-

TABLE VII.
Summary of Results from Calculation of Free Energy Differences (ΔG, kJ mol^{-1}).

	Methane		Ethane		Propane		Butane		Isobutane	
λ	t[a]	$\langle \partial V/\partial\lambda \rangle$	t[a]	$\langle \partial V/\partial\lambda \rangle$[b]	t[a]	$\langle \partial V/\partial\lambda \rangle$[b]	t[a]	$\langle \partial V/\partial\lambda \rangle$[b]	t[a]	$\langle \partial V/\partial\lambda \rangle$[b]
0.0	50	13.9 ± 0.2	50	21.7 ± 0.2	50	29.7 ± 0.2	50	38.2 ± 0.4	50	36.9 ± 0.3
0.1	50	11.3 ± 0.3	50	19.1 ± 0.2	50	26.6 ± 0.3	50	33.4 ± 0.4	50	33.0 ± 0.3
0.2	50	9.6 ± 0.4	50	16.3 ± 0.4	50	22.2 ± 0.4	50	29.2 ± 0.6	50	28.5 ± 0.5
0.3	50	7.3 ± 0.4	50	10.4 ± 0.7	50	18.3 ± 0.7	50	23.6 ± 0.7	50	24.5 ± 0.7
0.4	50	3.7 ± 0.5	50	8.4 ± 0.7	50	13.2 ± 0.9	50	20.5 ± 1.0	50	16.5 ± 0.8
0.5	50	−0.1 ± 1.0	50	2.7 ± 1.2	50	5.1 ± 1.4	50	11.2 ± 1.0	50	10.9 ± 1.2
0.55	50	−3.7 ± 1.1	50	−1.8 ± 1.3	50	2.9 ± 1.7	50	7.2 ± 1.8	50	4.1 ± 1.9
0.6	50	−10.5 ± 2.1	50	−10.2 ± 2.4	50	−4.3 ± 1.8	50	0.1 ± 2.7	50	−1.6 ± 1.7
0.65	50	−15.0 ± 1.7	50	−15.6 ± 2.0	50	−14.9 ± 2.9	50	−15.1 ± 3.0	50	−15.6 ± 2.6
0.7	100	−20.8 ± 2.5	50	−32.2 ± 4.1	100	−27.7 ± 3.5	100	−34.8 ± 3.2	100	−40.5 ± 4.4
0.75	150	−49.6 ± 3.2	200	−60.7 ± 4.7	200	−56.3 ± 4.0	250	−56.0 ± 3.3	200	−68.8 ± 3.7
0.775	150	−55.6 ± 2.8	250	−68.2 ± 4.5	200	−79.4 ± 4.8	350	−80.5 ± 4.4	250	−100.4 ± 4.8
0.8	100	−58.2 ± 2.6	150	−75.3 ± 4.5	250	−99.6 ± 5.1	350	−104.9 ± 5.0	350	−115.0 ± 4.7
0.825	100	−51.2 ± 1.5	150	−64.1 ± 4.3	150	−93.1 ± 4.9	150	−117.6 ± 5.8	200	−124.4 ± 4.6
0.85	50	−43.4 ± 1.6	50	−71.3 ± 2.2	50	−94.8 ± 4.8	200	−108.8 ± 3.3	200	−112.3 ± 3.2
0.9	50	−25.1 ± 0.7	50	−39.4 ± 1.8	50	−59.2 ± 1.5	50	−74.4 ± 2.2	50	−76.1 ± 2.1
0.95	50	−9.9 ± 0.4	50	−15.4 ± 1.4	50	−25.9 ± 1.0	50	−29.6 ± 1.6	50	−31.9 ± 1.1
1.0	50	−0.5 ± 0.3	50	−0.6 ± 0.4	50	−0.1 ± 0.8	50	−0.5 ± 0.7	50	−0.2 ± 0.8
ΔG		−8.0 ± 1.3		−9.2 ± 2.1		−9.0 ± 2.2		−7.7 ± 2.2		−10.4 ± 2.2

[a] Simulation time (t, ps) used for the averaging.
[b] $\langle \partial V/\partial\lambda \rangle$ in KJ mol^{-1}.

sures (NVT) or densities (NPT) of nine alkanes in the liquid state at 298 K (or at the boiling point in the case of methane). Excluding liquid ethane, for which no reasonable model could be derived at 298 K, the average deviation from the experiment for the computed enthalpies of vaporization (NPT simulations) is 0.6 kJ mol^{-1}, and for the computed densities it is 2.2%. As expected, the parametrization is dependent on the temperature and density of the model liquid alkanes studied. It has also been shown that the parametrization is highly dependent on the cutoff radius used for the truncation of (long-range) van der Waals interactions for cutoff radii between 0.8 and 1.4 nm for molecules such as butane, isobutane, and pentane. Of course, it is possible to parametrize a force field for such molecules using shorter cutoff radii for the van der Waals interactions. Later applications would, however, be bound to that cutoff and the parameters would be less transferrable. The effect of the cutoff radius is proportional to the number of atoms per molecule, as well as to the density of the liquid, because the enthalpy of vaporization and the vapor pressure are both functions of the number of interactions per molecule. A cutoff radius of 1.4 nm or greater is generally required to have a small cutoff dependence in the results. We have used a cutoff radius of 1.6 nm in the parametrization procedure (1.4 nm in the case of methane) to avoid the need for long-range (tail) corrections. Such corrections are not feasible in inhomogeneous systems such as a protein in water. The use of a computationally efficient twin-range cutoff of 0.8/1.4 nm for the van der Waals interactions has, however, given results equivalent to a single 1.4-nm cutoff.

The $C12_{ii}^{1/2}$ parameter of the water oxygen for interactions with nonpolar atoms has also been fitted to reproduce the experimental free energies of hydration of five of the alkanes studied: methane, ethane, propane, butane, and isobutane. The average deviation from the experiment for the computed free energies of hydration is 0.9 kJ mol^{-1}.

In conclusion, it is again noted that the parameters given here are empirical. They have been derived using a specific set of conditions to reproduce a specific set of properties. As with any empirical force field, the choice of temperature, treatment of long-range nonbonded interactions, pressure coupling scheme, and so on, are implicitly incorporated into the parametrization. This should be remembered when transferring force field parameters from one system to another.

Acknowledgment

Financial support obtained from the Swiss National Science Foundation (Project 21-41875.94) is gratefully acknowledged.

References

1. W. F. van Gunsteren and H. J. C. Berendsen, *Angew. Chem. Int. Ed. Engl.*, **29**, 992 (1990).
2. W. D. Cornell, A. E. Howard, and P. A. Kollman, *Curr. Opin. Struct. Biol.*, **1**, 201 (1991).
3. P. H. Hünenberger and W. F. van Gunsteren, In *Computer Simulation of Biomolecular Systems, Theoretical and Experimental Applications*, Vol. 3, W. F. van Gunsteren, P. K. Weiner, and A. J. Wilkinson, Eds., ESCOM Science Publishers b.v., Leiden, 1997, p. 3.
4. J. P. Bowen and N. L. Allinger, In *Reviews in Computational Chemistry*, K. B. Lipkowitz and D. B. Boyd, Eds., VCH Publishers Inc., New York, 1991, p. 81.
5. U. Dinur and A. T. Hagler, In *Reviews in Computational Chemistry*, K. B. Lipkowitz and D. B. Boyd, Eds., VCH Publishers Inc., New York, 1991, p. 99.
6. S. Lifson, A. T. Hagler, and P. Dauber, *J. Am. Chem. Soc.*, **101**, 5111 (1979).
7. A. T. Hagler, S. Lifson, and P. Dauber, *J. Am. Chem. Soc.*, **101**, 5122 (1979).
8. A. T. Hagler, P. Dauber, and S. Lifson, *J. Am. Chem. Soc.*, **101**, 5131 (1979).
9. A. T. Hagler, E. Huler, and S. Lifson, *J. Am. Chem. Soc.*, **96**, 5319 (1974).
10. F. A. Momany, L. M. Carruthers, R. F. McGuire, and H. A. Scheraga, *J. Phys. Chem.*, **78**, 1595 (1974).
11. F. A. Momany, R. F. McGuire, A. W. Burgess, and H. A. Scheraga, *J. Phys. Chem.*, **79**, 2361 (1975).
12. S. J. Weiner, P. A. Kollman, D. A. Case, U. C. Singh, C. Ghio, G. Alagona, S. J. Profeta, and P. Weiner, *J. Am. Chem. Soc.*, **106**, 765 (1984).
13. J. Hermans, H. J. C. Berendsen, W. F. van Gunsteren, and J. P. M. Postma, *Biopolymers*, **23**, 1513 (1984).
14. S. J. Weiner, P. A. Kollman, D. T. Nguyen, and D. A. Case, *J. Comput. Chem.*, **7**, 230 (1986).
15. D. J. Nelson and J. Hermans, *Biopolymers*, **12**, 1269 (1973).
16. D. R. Ferro and J. Hermans, In *Liquid Crystals and Ordered Fluids*, J. F. Johnson and R. Porter, Eds., Plenum, New York, 1970, p. 259.
17. D. Poland and H. A. Scheraga, *Biochemistry*, **6**, 3791 (1967).
18. H. J. C. Berendsen, J. P. M. Postma, W. F. van Gunsteren, and J. Hermans, In *Intermolecular Forces*, B. Pullman, Ed., D. Reidel Publishing Company, Dordrecht, 1981, p. 331.
19. W. L. Jorgensen, J. D. Madura, and C. J. Swenson, *J. Am. Chem. Soc.*, **106**, 6638 (1984).
20. G. Kaminski, E. M. Duffy, T. Matsui, and W. L. Jorgensen, *J. Phys. Chem.*, **98**, 13077 (1994).
21. W. L. Jorgensen, D. S. Maxwell, and J. Tirado–Rives, *J. Am. Chem. Soc.*, **118**, 11225 (1996).

22. W. F. van Gunsteren and H. J. C. Berendsen, *Groningen Molecular Simulation* (*GROMOS*) *Library Manual*, BIOMOS b.v., Groningen, 1987.
23. W. F. van Gunsteren, S. R. Billeter, A. A. Eising, P. H. Hünenberger, P. Krüger, A. E. Mark, W. R. P. Scott, and I. G. Tironi, *Biomolecular Simulation: The GROMOS96 Manual and User Guide*, vdf Hochschulverlag AG an der ETH Zürich and BIOMOS b.v., Zürich, Groningen, 1996.
24. L. G. Dunfield and A. W. Burgess, H. A. Scheraga, *J. Phys. Chem*., **82**, 2609 (1978).
25. J. P. M. Postma, Ph.D. thesis, University of Groningen, 1985.
26. H. J. C. Berendsen, J. P. M. Postma, W. F. van Gunsteren, A. DiNola, and J. R. Haak, *J. Chem. Phys*., **81**, 3684 (1984).
27. J. P. Ryckaert, G. Ciccotti, and H. J. C. Berendsen, *J. Comput. Phys*., **23**, 327 (1977).
28. W. F. van Gunsteren, T. C. Beutler, F. Fraternali, P. M. King, A. E. Mark, and P. E. Smith, In *Computer Simulation of Biomolecular Systems*, *Theoretical and Experimental Applications*, Vol. 2, W. F. van Gunsteren, P. K. Weiner, and A. J. Wilkinson, Eds., ESCOM Science Publishers b.v., Leiden, 1993, p. 315.
29. D. Fincham, N. Quirke, and D. J. Tildesley, *J. Chem. Phys*., **84**, 4535 (1986).
30. M. P. Allen and D. J. Tildesley, *Computer Simulation of Liquids*, Oxford University Press, New York, 1987.
31. M. R. Spiegel, *Theory and Problems of Statistics*, McGraw−Hill, New York, 1972.
32. W. L. Jorgensen, *BOSS Version 3.6*, Yale University, New Haven, CT, 1995.
33. *TRC Thermodynamic Tables−Hydrocarbons*, Texas A & M University System, College Station, TX.
34. W. L. Jorgensen, J. Chandrasekhar, J. D. Madura, R. W. Impey, and M. L. Klein, *J. Chem. Phys*., **79**, 926 (1983).
35. S. Cabani, P. Gianni, V. Mollica, and L. Lepori, *J. Solut. Chem*., **10**, 563 (1981).
36. A. Ben-Naim and Y. Marcus, *J. Chem. Phys*., **81**, 2016 (1984).